Preparation and reactivity of macrocyclic rhodium(III) alkyl complexes

Jack M. Carraher, Arkady Ellern, and Andreja Bakac*

Ames Laboratory and Chemistry Department, Iowa State University, Ames, IA 50011

*email: bakac@ameslab.gov

Abstract Macrocyclic rhodium(II) complexes $LRh(H_2O)^{2+}$ (L = L^1= cyclam and L^2 = *meso*-Me_6-cyclam) react with alkyl hydroperoxides $RC(CH_3)_2OOH$ to generate the corresponding rhodium(III) alkyls $L(H_2O)RhR^{2+}$ (R = CH_3, C_2H_5, $PhCH_2$). Methyl and benzyl complexes can also be prepared by bimolecular group transfer from alkyl cobaloximes $(dmgH)_2(H_2O)CoR$ and $(dmgBF_2)_2(H_2O)CoR$ (R = CH_3, $PhCH_2$) to the rhodium(II) complexes. The new organorhodium complexes exhibit great stability in aqueous solutions at room temperature, but undergo efficient Rh-C bond cleavage upon photolysis.

* email: bakac@ameslab.gov

Introduction

Spectroscopic and crystallographic characterization of rhodium(III) complexes is, in general, greatly facilitated by substitutional and redox inertness of Rh(III). Inorganic complexes of saturated N_4 macrocycles[1] clearly belong in this category and are considered especially robust. Recent work has shown, however, that this platform in combination with small molecules (O_2 and $^{\bullet}NO$) can be used to generate and stabilize complexes in nonstandard oxidation states. For example, the nitrosyl complex $L^2(H_2O)RhNO^{2+}$, formally a Rh(III) complex of NO^-, is oxidized by $Ru(bpy)_3^{3+}$ to $L^2(H_2O)RhNO^{3+}$, a $\{MNO\}^7$ species in Enemark-Feltham notation.[2] This compound is highly oxidizing ($E^0 = 1.31$ V)[3] and persists in acidic aqueous solutions for over a minute. The dioxygen analog, $L^2(H_2O)RhOO^{3+}$, was not observed directly, but its presence was inferred from the kinetics and products of the $L^2(H_2O)RhOOH^{2+}$ /I^- reaction.[4] It was concluded that $L^2(H_2O)RhOO^{3+}$ has a sufficiently long lifetime in aqueous solutions to engage in bimolecular reactions with reducing substrates.[4]

We have now extended our work with macrocyclic rhodium(III) to alkyl complexes. The goal is to prepare and characterize such compounds, and examine their reactivity in thermal reactions, especially those involving redox transformations, and as potential photochemical sources of alkyl radicals. Despite the abundance of alkylmetal complexes that release radicals upon photolysis, none of them are problem-free. Alkylcobaloximes, for example, release free $dmgH_2$ that precipitates from aqueous solutions and complicates spectroscopic studies. Also, $dmgH_2$ is not chemically inert and will engage in substitution and redox reactions with various substrates. Clearly, alkylrhodoximes[5,6] suffer from the same downsides as their cobalt analogs.

A series of macrocyclic cobalt complexes $L^1(H_2O)CoR^{2+}$ (L^1 = cyclam) produce alkyl radicals efficiently upon photolysis with visible light. Unfortunately, the benzyl complex is unstable and decays by thermal Co-C bond homolysis in seconds,[7] and branched alkyls (2-propyl, 2-butyl) were too unstable to isolate.[8] We have now prepared several alkylrhodium analogs, and found them to be quite stable under most conditions, as described below.

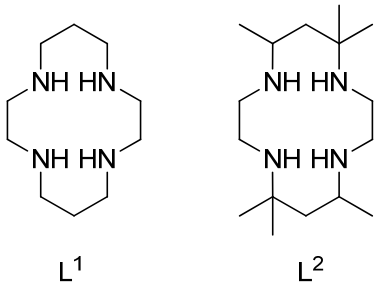

L^1 L^2

Experimental

Materials. Acidic aqueous solutions of $L(H_2O)Rh^{2+}$ complexes (L = L^1, L^2) were generated by photolysis of the corresponding hydrides $L(H_2O)RhH^{2+}$.[9] Solid perchlorate and trifluoromethanesulfonate salts of $L(H_2O)RhH^{2+}$ were prepared as described previously.[9] Alkyl cobalt complexes $(dmgH)_2(H_2O)CoR$ ($dmgH_2$ = dimethylglyoxime) and $(dmgBF_2)_2(H_2O)CoR$ were prepared by published procedures.[10] The hydroperoxides $C_2H_5C(CH_3)_2OOH$ and $PhCH_2C(CH_3)_2OOH$ were synthesized from the corresponding alcohols,[11] and $CH_3C(CH_3)_2OOH$ (70 % in H_2O) was purchased from Sigma-Aldrich. D_2O (99.9 % D) and $Cr(ClO_4)_3$,6 H_2O (both Sigma-Aldrich), NaCl, $NaClO_4$, and 70 % $HClO_4$ (all Fisher) were used as received. Water was purified with a Barnstead EASYpure III UV UF system.

Instrumentation. Photolyses were performed in standard 1-cm square fluorescence quartz cells in Luzchem LZC-5 photoreactor at 313 nm. Gaseous products were analyzed with an Agilent Technologies 7890A gas chromatograph equipped with an FID detector and a 0.320 mm I.D. capillary column (GS-GASPRO 113-4312, 15 m). Nitrogen flow rate was 25 cm^3/s. The split injector (1:40) was kept at 200 °C and FID detector at 350 °C. Initial oven temperature was 40 °C, increased by 10 °C/min, and held at a final temperature of 200 °C for 1 min. Prior to injection of the gas samples, the solutions were shaken vigorously to expel gases into the headspace. Standard mixtures of ethane, ethylene and butane in aqueous solution for GC calibration were prepared by the reaction of *tert*-amyl hydroperoxide and excess $Fe(H_2O)_6^{2+}$ as described previously.[12] UV-Vis spectra and kinetic data were collected with a Shimadzu UV-3101PC spectrophotometer. Kinetic data were fitted with KaleidaGraph 4.0 software.

^1H NMR spectra were collected with a Bruker 600 MHz NMR (AVIII600). Heteronuclear Single Quantum Coherence (HSQC) spectra were acquired with 256 slices at 8 scans per slice for a total acquisition time of 5.1 ms. Elemental (C, H, N) analysis used a PE 2100 Series II combustion analyzer (Perkin Elmer Inc., Waltham, MA) with acetanilide standard (Perkin Elmer). Combustion and reduction temperatures were 925 °C and 640 °C. The precision for each element is ± 0.3 %. Rhodium concentrations for the determination of molar absorptivities were obtained by ICP-MS Element 1 by Thermo Finnigan.

Preparation of $L(H_2O)RhR^{2+}$ Complexes. Millimolar solutions of $L(H_2O)RhR^{2+}$ (L = L^1, L^2) were generated from $RC(CH_3)_2OOH$ (R = CH_3, C_2H_5, $PhCH_2$) and two equivalents of $L(H_2O)Rh^{2+}$ in 1-2 mM concentration range. Alkylrhodium products were

purified by cation exchange on Sephadex C-25 and eluted with 0.4 M $HClO_4$ or 0.4 M CF_3SO_3H. The yields were typically 30-40 %, but increased up to 70% in spectrophotometric titrations with more dilute solutions.

*$L^1(H_2O)RhCH_3^{2+}$ (*solution*)* UV λ_{max}/nm (ε/$M^{-1}cm^{-1}$): 260 (300), 297 (310), Figure S1. ^{1}H NMR (600 MHz, 298 K, D_2O, pH 6.8): δ 4.46 (br s N*H*), 4.17 (br s N*H*), 3.34 (m), 3.20 (m), 2.99 (m), 2.86 (m), 2.65 (m), 2.19 (m), 1.69 (q), 1.18 (d, ^{1}J[Rh,H] = 2.4 Hz, Rh-*CH_3*), Figure S2. Two minor isomeric methyl rhodium species are also present, with Rh-*CH_3* resonances at 1.14 (d) and 1.08 (d), see later.

*$L^1(H_2O)RhCH_2CH_3^{2+}$ (*solution*)* UV λ_{max}/nm (ε/$M^{-1}cm^{-1}$): 261 (440), 301 (sh, 290), Figure 1. ^{1}H NMR (600 MHz, 298 K, D_2O): δ 3.36 – 2.68 (m), 2.32 (m), 2.21 (m), 1.98 (br m, Rh-*CH_2*-CH_3), 1.82 (m), 0.73 (t, Rh-CH_2-*CH_3*), Figure S3. The triplet at 0.68 ppm is for Rh-CH_2-*CH_3* of an isomeric ethyl rhodium species, see later.

$[L^1(H_2O)RhCH_2Ph](ClO_4)_2$ Anal. Calcd for $C_{17}H_{33}N_4RhCl_2O_9$: C, 33.40; H, 5.44; N, 9.17. Found: C, 33.28; H, 4.95; N, 8.92. UV (0.1 M $HClO_4$) λ_{max} / nm (ε/M^{-1} cm^{-1}): 258 (14000), Figure S4. ^{1}H NMR (600 MHz, 298 K, D_2O): δ 7.30 – 7.39 (m, Rh-CH_2-*C_6H_5*), 4.34 (s, N*H*), 3.98 (s, N*H*), 3.37 (dd, Rh-*CH_2*-Ph), 3.22 (d), 3.09 (m), 3.00 (m), 2.83 (m), 2.66 (m), 2.22 (br s), 2.11 (m), 1.94 (d), 1.73 (m), 1.25 (q). ^{13}C NMR (600 MHz, 298 K, D_2O, pH 6.8: δ 52.96, 51.11, 46.75, 42.71, 28.97, 24.79 (macrocyclic ligand), 18.45 (Rh-*CH_2*-Ph), 126.46, 128.20 and 130.31 (Rh-CH_2-*C_6H_5*). The cross peaks in HSQC spectra of $L^1(H_2O)RhCH_2Ph^{2+}$ and $L^1(H_2O)RhH^{2+}$, Figure S5, clearly identify chemical shifts of the benzyl group and the cyclam ligand in the aliphatic range.

[$L^2(H_2O)RhCH_3$]$(ClO_4)_2$ Anal. Calcd for ($RhC_{17}H_{41}N_4Cl_2O_9$): C, 33.02; H, 6.52; N, 9.06. Found: C, 32.69; H, 6.46; N, 8.96. UV λ_{max}/nm (ε/M^{-1} cm^{-1}): 268 (360), 301 (360), Figure S1. ^{1}H NMR (600 MHz, 298 K, D_2O): δ 4.05 (br s, N*H*), 3.97 (br s, N*H*), 3.66 (d), 3.21 (m), 3.13 (m), 2.99 (m), 2.20 – 2.60 (m), 1.82 (dd), 1.62 (m), 1.54 (m), 1.33 (s, 6H Rh-*CH_3* and L^2-*CH_3*), 1.31 (s, 3H), 1.27 (s, 3H), 1.26 (s, 3H), 1.21 (d, 3H), 1.19 (s, 3H), Figure S6. The spectrum of $L^2(H_2O)RhH^{2+}$ is shown for comparison in Figure S7.

Preparation of $L(H_2O)RhR^{2+}$ by alkyl group transfer A solution of $L^1(H_2O)RhCH_2Ph^{2+}$ was prepared by addition of 100 mL of 2 mM $L(H_2O)Rh^{2+}$ to 0.1 g (ca 3 mmol) of solid $(dmgH)_2(H_2O)CoCH_2Ph$ or $(dmgBF_2)_2(H_2O)CoCH_2Ph$. The mixture was allowed to react 18 hours in the dark under argon, followed by filtration to remove solid $dmgH_2$ or $Co(dmgBF_2)_2$. The product $L^1(H_2O)RhCH_2Ph^{2+}$ was purified by cation exchange on Sephadex C25, eluted with 0.4 M $HClO_4$ and concentrated by rotary evaporation. Addition of $NaClO_4$ yielded the white solid of $[L^1(H_2O)RhCH_2Ph](ClO_4)_2$ which was filtered and air-dried. Yield: 17%.

Solutions of $L^1(H_2O)RhCH_3^{2+}$ and $L^2(H_2O)RhCH_3^{2+}$ were prepared by a method analogous to that used for $L^1(H_2O)RhCH_2Ph^{2+}$ except that methyl transfer from $(dmgH)_2(H_2O)CoCH_3$ required much less time. The yield of methylrhodium complexes was 80 %. Salts of $L^1(H_2O)RhCH_3^{2+}$ were too soluble in water to be isolated as solids, but $[L^2(H_2O)RhCH_3](CF_3SO_3)_2$ precipitated upon addition of solid $LiCF_3SO_3$ to a concentrated solution. The white crystals were washed with CH_2Cl_2, hexanes and ice-cold water, and air-dried. The UV-Vis and ^{1}H NMR spectra were identical to those given above for the compounds obtained by the hydroperoxide method.

Crystal growth and structure determination. A solid sample of $[L^2(H_2O)RhCH_3](CF_3SO_3)_2$ (20 mg) was dissolved in warm 0.001 M $HClO_4$. The solution was cooled, filtered, and transferred to an NMR tube. Good quality crystals of $[L^2(H_2O)RhCH_3](ClO_4)_2$ grew in a refrigerator in four days. Crystals of $[L^1(H_2O)RhCH_2Ph](ClO_4)_2$ were obtained by rotary evaporation of an ion-exchanged solution. Addition of $NaClO_4$ caused the precipitation of $[L^1(H_2O)RhCH_2Ph](ClO_4)_2$, which was then redissolved in a minimum amount of warm water (~ 30 °C) and allowed to crystallize in a refrigerator.

A crystal suitable for X-Ray analysis was selected under the microscope and covered with PARATONE oil. The sample was mounted in a diffractometer under the stream of cold nitrogen. The full sphere X-ray intensity data were measured till resolution 0.71 Å (0.5 deg. width ω -scan, 15 sec per frame) using BRUKER APEX2 CCD diffractometer. The frames were integrated using a narrow-frame algorithm. Data were corrected for absorption effects using the multi-scan method (SADABS). All non-hydrogen atoms were refined in full-matrix anisotropic approximation based on F^2 . All expected hydrogen atoms were placed on a calculated positions and were refined in isotropic approximation using "riding" model. The U_{iso}(H) values have been set at 1.2 - 1.5 times the U_{eq} value of the carrier atom. All calculations were performed using APEX II software suite.[13] CCDC 938294-938295 contains the supplementary crystallographic data for this paper. These data can be obtained free of charge from The Cambridge Crystallographic Data Centre via www.ccdc.cam.ac.uk/data_request/cif

X-ray crystal structures for the cations *trans*-$[L^2(H_2O)RhCH_3]^{2+}$ and *trans*-$[L^1(H_2O)RhCH_2Ph]^{2+}$ are shown in Figures 2 and 3, respectively.

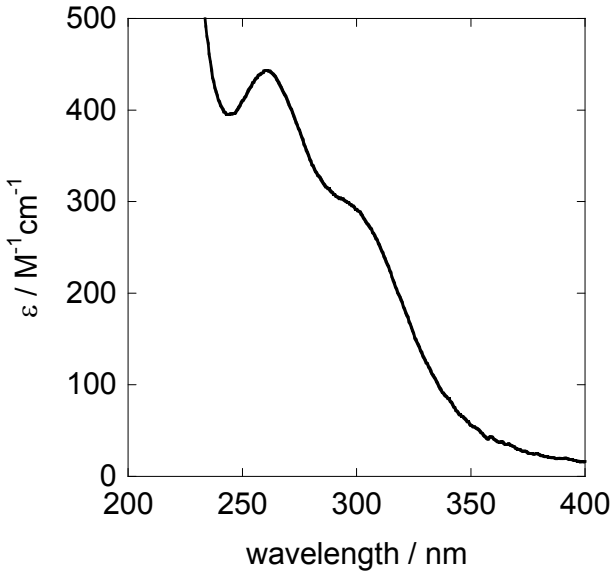

Figure 1. UV spectrum of $L^1(H_2O)RhC_2H_5^{2+}$ in acidic aqueous solution.

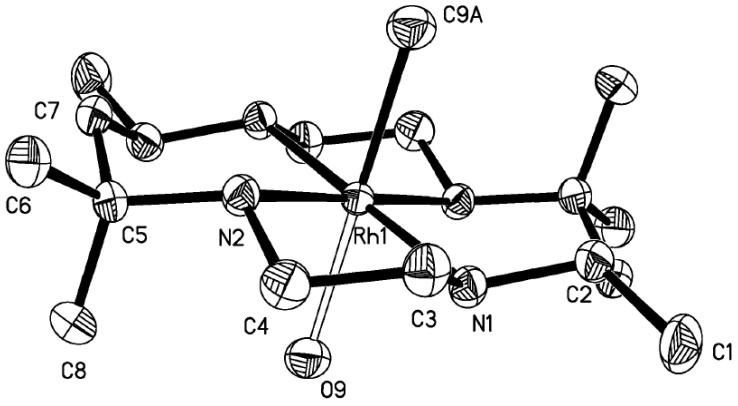

Figure 2. ORTEP drawing of the cation *trans*-$[L^2(H_2O)RhCH_3]^{2+}$ at 50 % probability level. Hydrogen atoms are not shown. Bond lengths/Å: Rh1-N1, 2.073(2); Rh1-N2, 2.090(2); Rh1-C9A, 2.216(3); Rh1-O9, 2.216(3). Angles/deg: N1-Rh1-N2, 84.62(9); N1-Rh1-O9, 93.57(10); N1-Rh1-C9A, 86.43(10); N2-Rh1-O9, 84.96(10); N2-Rh1-C9A, 95.04(10).

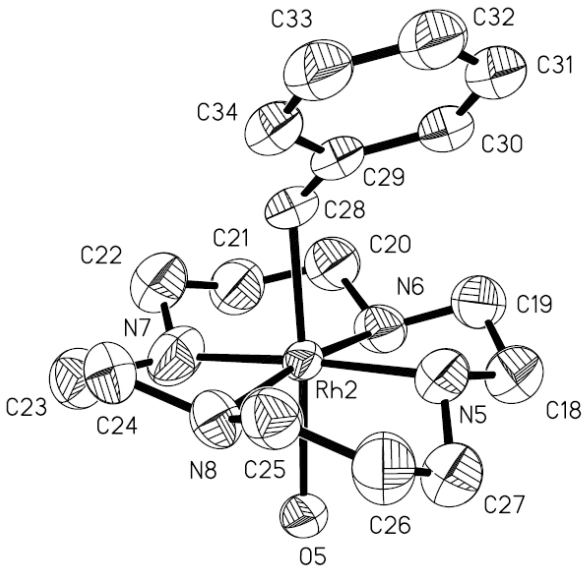

Figure 3. ORTEP drawing of the cation *trans*-$[L^1(H_2O)RhCH_2Ph]^{2+}$ at 50 % probability level. Hydrogen atoms are not shown. Bond lengths/Å: Rh2-N5, 2.055(7); Rh2-N6, 2.057(6); Rh2-N7, 2.045(8); Rh2-N8 2.050(6); Rh2-C28, 2.106(7); Rh2-O5, 2.299(5); C28-C29, 1.472(12). Angles/deg: N5-Rh2-N7, 176.0(3); N5-Rh2-N8, 94.5(3); N6-Rh2-N7, 93.8(3); N5-Rh2-C28, 91.7(3); O5-Rh2-C28, 173.7(3); Rh2-C28-C29, 122.9(5).

Results and Discussion

Reactions of $L(H_2O)Rh^{2+}$ with alkyl hydroperoxides. The reactions between submillimolar concentrations of $CH_3C(CH_3)_2OOH$ and $L(H_2O)Rh^{2+}$ (L = L^1, L^2) were nearly complete in mixing time. All of the observations are consistent with the sequence in eq 1-2 written in analogy with reactions of other reduced transition metal complexes, but encumbered with side reactions owing to the low concentrations of photochemically generated $L(H_2O)Rh^{2+}$. Slightly more than two equivalents of $L(H_2O)Rh^{2+}$ per mole of hydroperoxide were consumed, as determined from the UV-Vis spectra acquired during titration.

$$L(H_2O)Rh^{2+} + CH_3C(CH_3)_2OOH + H^+ \rightarrow LRh(H_2O)_2^{3+} + {}^{\bullet}CH_3 + (CH_3)_2CO \quad (1)$$

$$L(H_2O)Rh^{2+} + {}^{\bullet}CH_3 \rightarrow L(H_2O)RhCH_3^{2+} \quad \text{fast} \quad (2)$$

As already commented in Experimental, the yields of $L(H_2O)RhCH_3^{2+}$ were smaller than expected for the ideal 2:1 stoichiometry of eq 1-2. Also, methane and ethane were identified by GC immediately after completion of the reaction. The ratio of the two alkanes was somewhat dependent on absolute concentrations of the reagents, and on the length of time that $L(H_2O)RhH^{2+}$ was photolyzed to generate $L(H_2O)Rh^{2+}$. The observed gaseous products were most likely formed by radical dimerization and hydrogen abstraction from $L(H_2O)RhH^{2+}$ [14] and/or $CH_3C(CH_3)_2OOH$.[15]

The reaction of $L^1(H_2O)Rh^{2+}$ with $C_2H_5C(CH_3)_2OOH$ exhibited an approximate 3:1 stoichiometry. Ethane, ethylene and traces of butane were formed in addition to $L^1(H_2O)RhC_2H_5^{2+}$. The ratio, $[C_2H_6]:[C_2H_4]:[C_4H_{10}]$ = 1:0.3:0.004, differs significantly from that expected for ethyl radical self-reaction (1:1:0.35).[16] The source of ethane is again believed to be hydrogen atom abstraction from the hydroperoxide and/or rhodium hydride, eq 3 and 4. Hydrogen atom transfer in the opposite direction, i.e. from ethyl radicals to $L^1(H_2O)Rh^{2+}$, eq 5, is the most plausible source of C_2H_4. This reaction also regenerates the hydride which reenters reaction 4. Radical self-reaction is unimportant as judged by negligible amounts of butane. Similarly, the $L^1(H_2O)Rh^{2+}/PhCH_2C(CH_3)_2OOH$ reaction yielded no bibenzyl, the main product of the self-reaction of benzyl radicals.

$${}^{\bullet}C_2H_5 + HOO(CH_3)_2CC_2H_5 \rightarrow C_2H_6 + {}^{\bullet}OO(CH_3)_2CC_2H_5 \quad (3)$$

$${}^{\bullet}C_2H_5 + L^1(H_2O)RhH^{2+} \rightarrow C_2H_6 + L^1(H_2O)Rh^{2+} \quad (4)$$

$${}^{\bullet}C_2H_5 + L^1(H_2O)Rh^{2+} \rightarrow C_2H_4 + L^1(H_2O)RhH^{2+} \quad (5)$$

Reactions of $L(H_2O)Rh^{2+}$ with cobalt alkyls. Yellow solutions of submillimolar $(dmgH)_2(H_2O)CoCH_3$ turned colorless immediately upon mixing with equimolar amounts of $L^1(H_2O)Rh^{2+}$. This color change is associated with rapid methyl group transfer from cobalt to $L^1(H_2O)Rh^{2+}$, eq 6.[17] The 1:1 stoichiometry was determined from the absorbance decrease at the 440-nm maximum of $(dmgH)_2(H_2O)CoCH_3$.

The product solutions exhibited shoulders near 300 nm and 340 nm, and intense absorption below 300 nm attributable to free $dmgH_2$ formed by dissociation from Co(II), eq 7. As shown above, the shoulder at 300 nm is associated with the Rh-alkyl bond. The 340 nm feature is characteristic for a species generated from $L^1(H_2O)Rh^{2+}$ and $dmgH_2$ in a slow step following methyl transfer in experiments with excess $L^1(H_2O)Rh^{2+}$.[17] This species is extremely stable both thermally and photochemically, and did not interfere with the chemistry of interest.

$$L^1(H_2O)Rh^{2+} + (dmgH)_2(H_2O)CoCH_3 \rightarrow L^1(H_2O)RhCH_3^{2+} + Co(dmgH)_2 \qquad (6)$$

$$Co(dmgH)_2 + 2H^+ + 6H_2O \rightarrow Co(H_2O)_6^{2+} + 2\ dmgH_2 \qquad \text{fast} \qquad (7)$$

In some experiments, $(dmgH)_2(H_2O)CoCH_3$ was replaced with $(dmgBF_2)_2(H_2O)CoCH_3$.[18] Alkyl transfer from the latter generates $(dmgBF_2)_2Co(H_2O)_2$ which does not dissociate dioxime ligands and was therefore expected to generate products free of the 340-nm species. None the less, small amounts of this species were still observed. In subsequent preparations, the $(dmgBF_2)_2(H_2O)_2Co$ product was removed by filtration as soon as the reaction was over to minimize its availability in follow-up chemistry.

Benzylcobaloxime also reacts with $L^1(H_2O)Rh^{2+}$ by alkyl group transfer, but the reaction is quite slow. Owing to long reaction times (about 18 hours for millimolar concentrations of both reactants) and extreme air-sensitivity of small concentrations of $L^1(H_2O)Rh^{2+}$, the yields of $L^1(H_2O)RhCH_2Ph^{2+}$ were poor (17 %).

Reactions of $L^1(H_2O)Rh^{2+}$ with ethyl, isopropyl, and isobutyl cobaloximes were completed in several minutes or less, but did not produce alkyl rhodium complexes. As described elsewhere,[17] those reactions take place by hydrogen atom transfer from the alkyl group and produce rhodium hydride and a-olefins.

NMR spectra. ^{1}H NMR of $L^1(H_2O)RhCH_3^{2+}$ is shown in Figure S2. The methyl group appears as a doublet at 1.18 ppm. There are also two weak doublets at 1.08 ppm and 1.13 ppm that persist through multiple recrystallizations of the perchlorate salt and do not change even after prolonged aging of the NMR solutions. We associate these signals with small amounts of isomeric methylrhodium complexes containing the macrocyclic ligand in different conformations.[19-21] The change in stereochemistry around nitrogen most likely takes place at the rhodium(II) stage, similar to other cases of conformational changes that occur at labile metal centers.[22,23] The parent hydride exhibits only one doublet in the hydride region, confirming the presence of a single, RRSS conformer,[24] Figure S8.

The aliphatic region in ^{1}H NMR spectrum of $L^2RhCH_3^{2+}$ is similar to that of L^2RhH^{2+}. The signal for Rh-*CH*$_3$ is at 1.33 ppm and coincides with the signal for one of the six ligand *CH*$_3$ groups, as deduced from integration ratios. Also, the entire 1.19 – 2.35 ppm region integrates to 18 H for L^2RhH^{2+}, and 21 H for $L^2RhCH_3^{2+}$.

The resonances for ethyl group in $L^1RhC_2H_5^{2+}$ are found at 0.73 ppm (t, CH_3), and 1.98 ppm (br, CH_2), Rh-$\underline{CH_2}$-CH_3, Figure S3. The weak resonance at 0.68 ppm is again attributed to an isomeric ethyl rhodium species. In the related ethyl rhodoxime, the ethyl signals are shifted upfield (1.24 ppm, dq, 2H, Rh-$\underline{CH_2}$-CH_3, and 0.59 ppm, dt, 3H, Rh-CH_2-$\underline{CH_3}$)[5] owing to unsaturation in the equatorial ligand.

The $\underline{CH_2}$-Ph signals for $L^1RhCH_2Ph^{2+}$ appear as doublets at 3.27 and 3.24 ppm. This assignment is confirmed by the cross peaks in HSQC spectra, Figure S5. The appearance of two doublets is attributed to hindered rotation around the Rh-C bond in this sterically congested complex, similar to the case of 2-naphthyl and 2-bromo-benzyl cobaloximes at lower temperature.[25]

Reactivity of LRhR^{2+}. UV-vis spectra of $L(H_2O)RhR^{2+}$ solutions remained unchanged over several days at room temperature or for at least 18 hours at 60 °C in either argon or oxygen atmosphere in the dark. Also, there was no indication of even trace amounts of gaseous products by GC. Several minutes of irradiation of air-free solutions of sub-millimolar $L^1(H_2O)RhCH_3^{2+}$ at 313 nm also produced virtually no change in the UV-Vis spectrum, but when the photolysis was conducted in an oxygen atmosphere, large amounts of $L^1(H_2O)RhOO^{2+}$ (λ_{max} = 267 nm, $\varepsilon = 9 \times 10^3$ $M^{-1}cm^{-1}$)[26] were formed. These results clearly identify the photochemical reaction as Rh-C bond homolysis as in eq 8. In the absence of scavengers the two fragments combine to regenerate $L^1(H_2O)RhCH_3^{2+}$, but under aerobic conditions, $L^1(H_2O)Rh^{2+}$ and $^{\bullet}CH_3$ are rapidly converted to $L^1(H_2O)RhOO^{2+}$ and non-absorbing short-lived $CH_3OO^{\bullet}$, respectively.

$$L^1RhCH_3^{2+} \overset{h\nu}{\rightleftharpoons} L^1Rh^{2+} + {}^{\bullet}CH_3 \xrightarrow{O_2,\text{fast}} L^1RhOO^{2+} + CH_3OO^{\bullet} \rightarrow \text{Prod.} \quad (8)$$

The photolysis of $L^1(H_2O)RhR^{2+}$ (R = ethyl, benzyl) under Ar in the presence of a large excess of $Cr(H_2O)_6^{2+}$ produced the respective alkyl chromium complexes, $(H_2O)_5CrC_2H_5^{2+}$ and $(H_2O)_5CrCH_2Ph^{2+}$. These data again support the homolysis followed by rapid capture of alkyl radicals by $Cr(H_2O)_6^{2+}$. In an analogous experiment with $L^1(H_2O)RhCH_3^{2+}$, however, no net loss of the alkylrhodium was observed. This result is easily explained by the rapid methyl group transfer to rhodium from the newly formed $(H_2O)_5CrCH_3^{2+}$ ($k > 10^3$ M^{-1} s^{-1})[17] to regenerate the starting materials in the sequence of events shown in eq 9.

$$L^1RhCH_3^{2+} \xrightarrow{h\nu,\ Cr^{2+}} L^1Rh^{2+} + CrCH_3^{2+} \xrightarrow{fast} L^1RhCH_3^{2+} + Cr^{2+} \qquad (9)$$

The newly prepared alkyl rhodium complexes are quite robust and persist in aqueous solutions for long periods of time. The analogous methyl and ethyl cobalt complexes are also stable, but $L^1(H_2O)CoCH_2Ph^{2+}$ homolyzes in seconds, $k_{hom} = 0.09$ s^{-1} at 25 °C.[7] The much more stable benzyl rhodium complex is a useful photochemical precursor of benzyl radicals.

Acknowledgements We are grateful to Dr. Veysey for help with elemental analysis, Dr. Cady for assistance with HSQC experiments, and to Jonna Berry and Dr. Houk for help with ICP experiments. This research is supported by the U.S. Department of Energy, Office of Basic Energy Sciences, Division of Chemical Sciences, Geosciences, and Biosciences through the Ames Laboratory. The Ames Laboratory is operated for the U.S. Department of Energy by Iowa State University under Contract DE-AC02-07CH11358.

Supporting Information: Crystallographic information and UV-Vis and NMR spectra of alkylrhodium complexes

References

(1) Bounsall, E. J.; Koprich, S. R. *Can. J. Chem.* **1970**, *48*, 1481-1491.
(2) Enemark, J. H.; Feltham, R. D. *Coord. Chem. Rev.* **1974**, *13*, 339-406.
(3) Kristian, K. E.; Song, W.; Ellern, A.; Guzei, I. A.; Bakac, A. *Inorg. Chem.* **2010**, *49*, 7182-7187.
(4) Szajna-Fuller, E.; Bakac, A. *Inorg. Chem.* **2007**, *46*, 10907-10912.
(5) Asaro, F.; Costa, G.; Dreos, R.; Pellizer, G.; von Philipsborn, W. *J. Organomet. Chem.* **1996**, *513*, 193-200.
(6) Giese, B.; Kesselheim, C.; Hartung, J.; Lindner, H. J.; Svoboda, I. *Chem. Ber.* **1993**, *126*, 1193-1200.
(7) Bakac, A.; Espenson, J. H. *Inorg. Chem.* **1987**, *26*, 4305-4307.
(8) Bakac, A.; Espenson, J. H. *Inorg. Chem.* **1987**, *26*, 4353-4355.
(9) Bakac, A.; Thomas, L. M. *Inorg. Chem.* **1996**, *35*, 5880-5884.
(10) Schrauzer, G. N.; Windgassen, R. J. *J. Am. Chem. Soc.* **1966**, *88*, 3738-3743.
(11) Milas, N. A.; Surgenor, D. M. *J. Am. Chem. Soc.* **1946**, *68*, 643-644.
(12) Carraher, J. M.; Pestovsky, O.; Bakac, A. *Dalton Transactions* **2012**, *41*, 5974-5980.
(13) APEX2 Version 4.1 (Bruker AXS Inc.,Madison WI, 2013).
(14) Bakac, A. *Inorg. Chem.* **1998**, *37*, 3548-3552.
(15) Bakac, A. *Inorg. React. Mech.* **1998**, *1*, 65.
(16) Bakac, A.; Espenson, J. H. *J. Phys. Chem* **1986**, *90*, 325-327.
(17) Carraher, J. M.; Bakac, A. *Submitted*.
(18) Gjerde, H. B.; Espenson, J. H. *Organometallics* **1982**, *1*, 435-440.
(19) Bosnich, B.; Poon, C. K.; Tobe, M. L. *Inorg. Chem.* **1965**, *4*, 1102-1108.
(20) Curtis, N. F. *Coord. Chem. Rev.* **2012**, *256*, 878-895.
(21) Barefield, E. K.; Bianchi, A.; Billo, E. J.; Connolly, P. J.; Paoletti, P.; Summers, J. S.; Van, D. D. G. *Inorg. Chem.* **1986**, *25*, 4197-4202.
(22) Moore, P.; Sachinidis, J.; Willey, G. R. *J. Chem. Soc., Chem. Commun.* **1983**, 522-523.
(23) Bakac, A.; Espenson, J. H. *J. Am. Chem. Soc.* **1986**, *108*, 713-719.
(24) Lemma, K.; Ellern, A.; Bakac, A. *Inorg. Chem.* **2003**, *42*, 3662-3669.
(25) Mandal, D.; Gupta, B. D. *Organometallics* **2006**, *25*, 3305-3307.
(26) Bakac, A. *J. Am. Chem. Soc.* **1997**, *119*, 10726-10731.

Supporting Information

Preparation and reactivity of macrocyclic rhodium(III) alkyl complexes

Jack M. Carraher, Arkady Ellern, and Andreja Bakac*

Ames Laboratory and Chemistry Department, Iowa State University, Ames, IA 50011

*email: bakac@ameslab.gov

Table of Contents

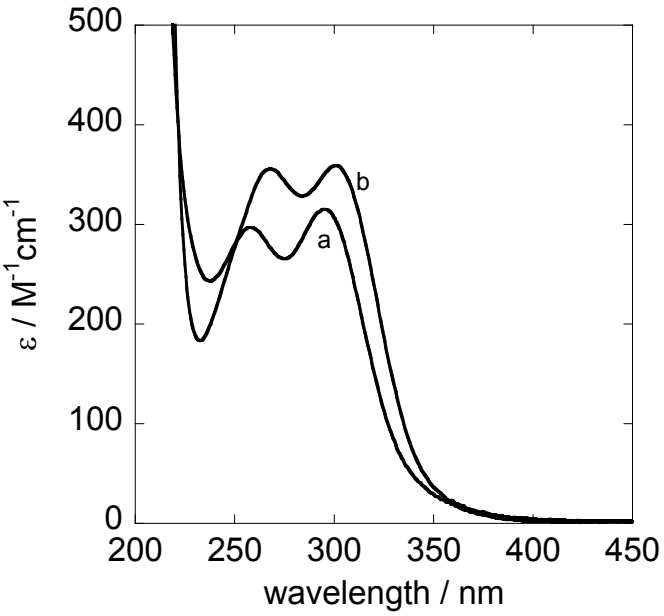

Figure S1. UV spectra of $L^1(H_2O)RhCH_3^{2+}$ (a) and $L^2(H_2O)RhCH_3^{2+}$ (b) in acidic aqueous solution.

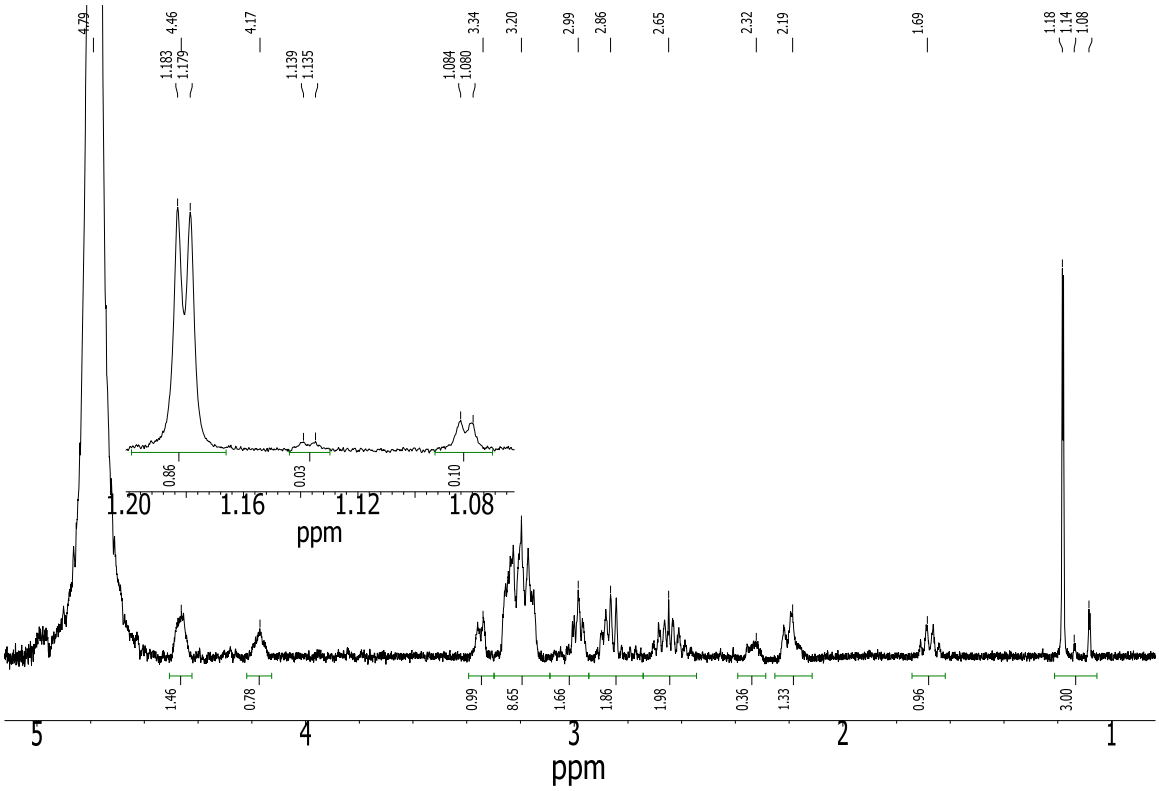

Figure S2. ^{1}H NMR of L^{1}RhCH$_3^{2+}$, 600 MHz, D_2O. Inset: Rh-$\underline{CH_3}$ isomers 1.18 ppm, 1.14 ppm, and 1.08 ppm. ^{1}J[Rh,H] = 2.4 Hz

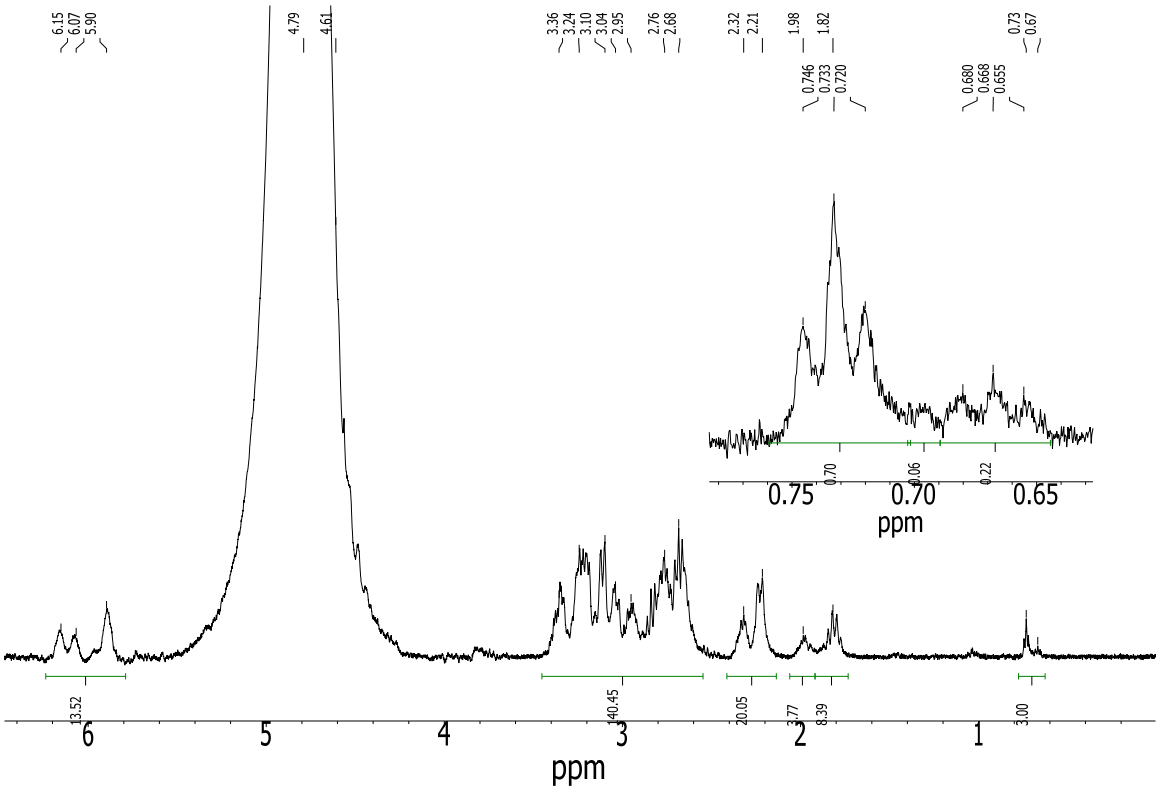

Figure S3. ^{1}H NMR of $L^{1}(H_2O)RhCH_2CH_3^{2+}$, 600 MHz, D_2O, after reaction between $L^{1}(H_2O)Rh^{2+}$ and $C_2H_5C(CH_3)_2OOH$ (contains $L^{1}(H_2O)Rh^{3+}$). 1.98 ppm (Rh-$\underline{CH_2}$-CH_3) and 0.73 & 0.67 ppm (Rh-CH_2-$\underline{CH_3}$) disappear upon UV photolysis under O_2.

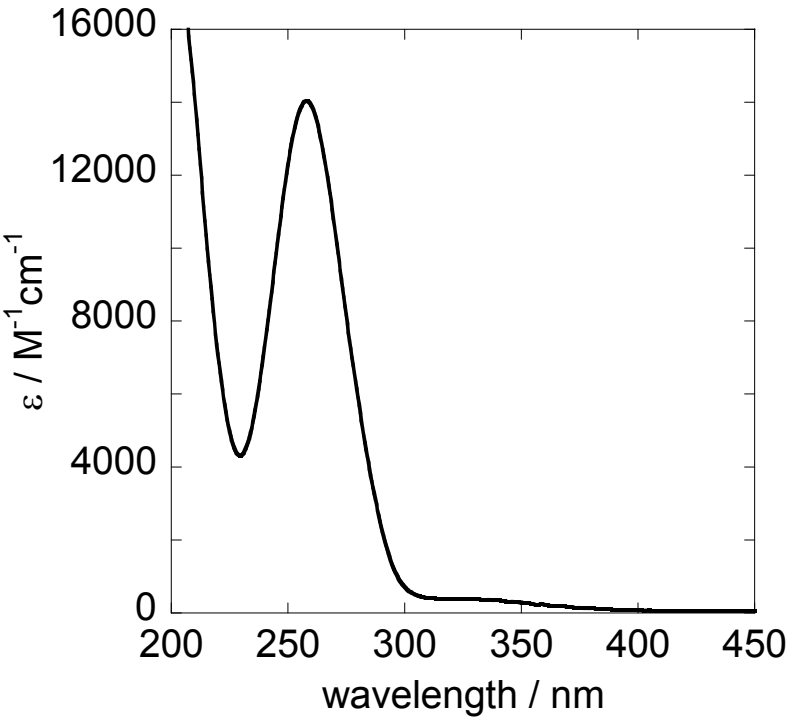

Figure S4. UV spectrum of $L^1(H_2O)RhCH_2C_6H_5^{2+}$ in acidic aqueous solution.

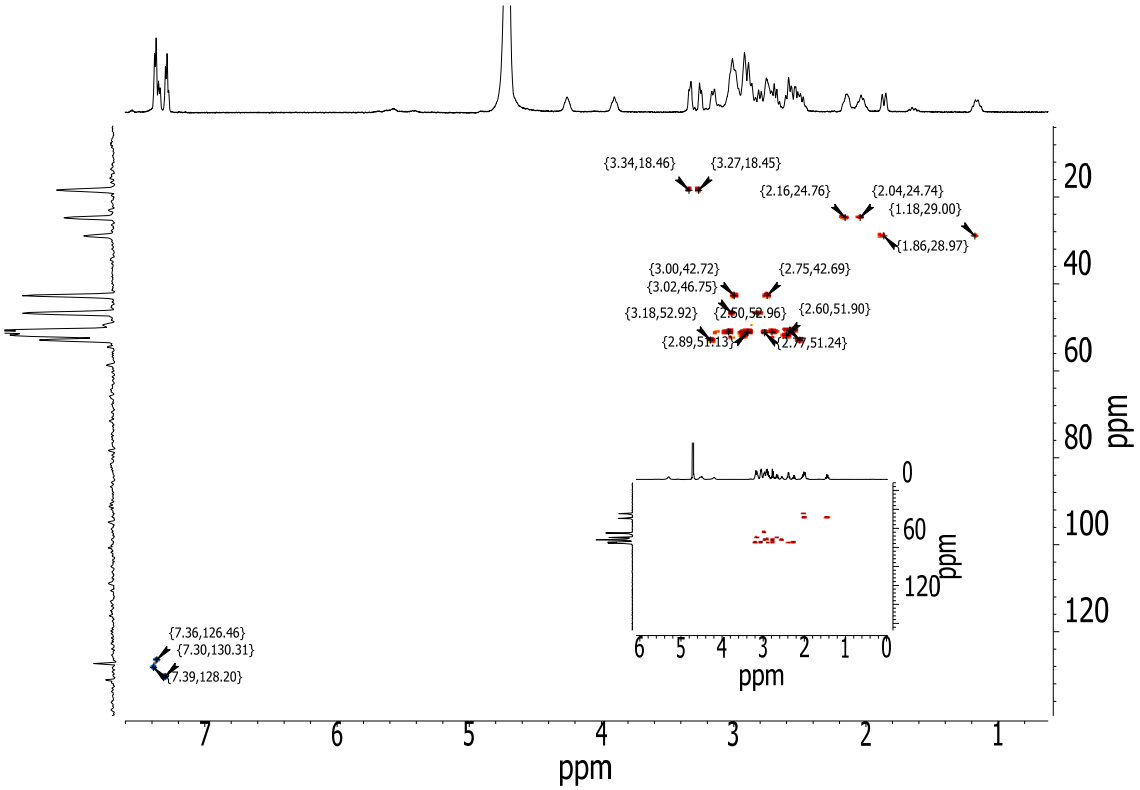

Figure S5. HSQC spectrum of of $L^1(H_2O)RhCH_2Ph^{2+}$, 600 MHz, D_2O. ^1H NMR (horizontal), ^{13}C projection (vertical). Inset: HSQC spectrum of $L^1(H_2O)RhH^{2+}$. Rh-$\underline{CH_2}$-Ph signals: ^1H 3.27, 3.34 ppm, ^{13}C 18.45 ppm. Rh-CH_2-$\underline{Ph}$ signals: ^1H 7.30-7.39 ppm, ^{13}C 126.46 – 130.31 ppm.

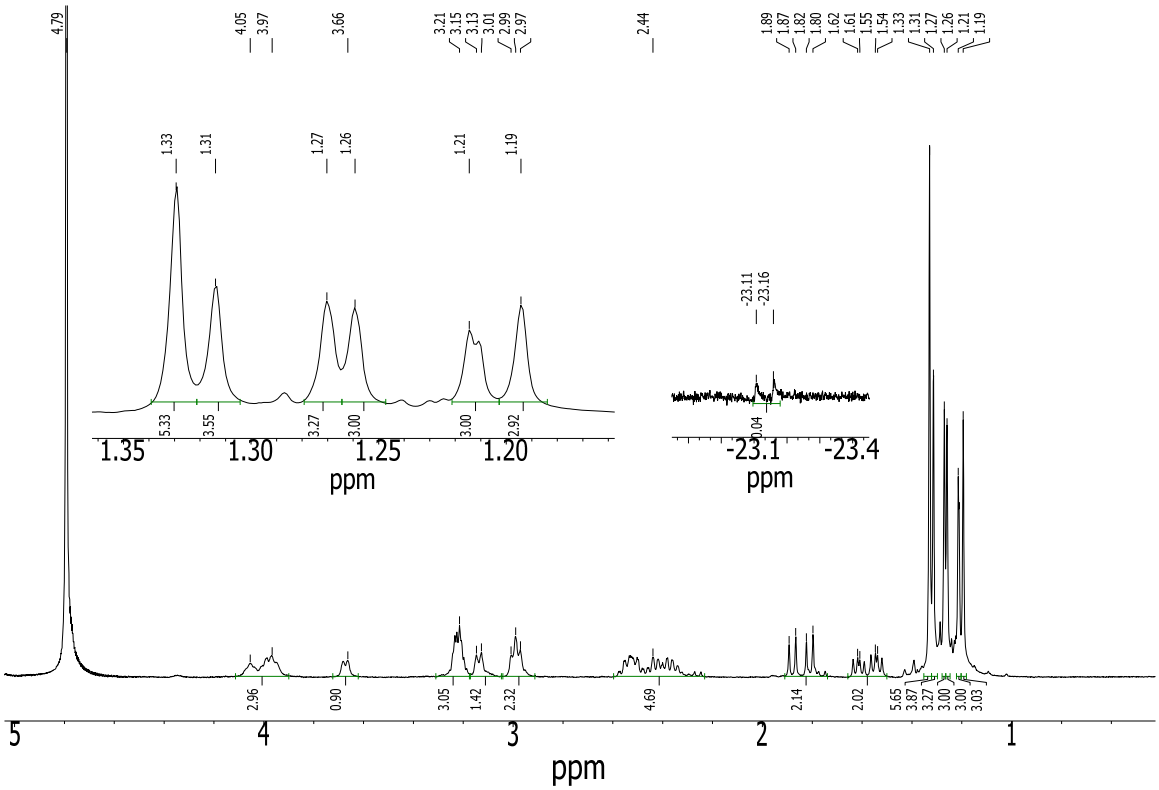

Figure S6. ^{1}H NMR of $L^{2}(H_2O)RhCH_3^{2+}$, 600 MHz, D_2O. Left inset: Ligand-CH_3 groups + Rh-CH_3 (1.33 ppm). There are 21 hydrogens in the 1.20 – 1.35 ppm region for $L^{2}(H_2O)RhCH_3^{2+}$, and 18 in the same region for $L^{2}(H_2O)RhH^{2+}$, Figure S7. Right inset: Rh-H region shows traces of remaining $L^{2}(H_2O)RhH^{2+}$ that was used as a starting material in the prep of the methyl complex, see Experimental.

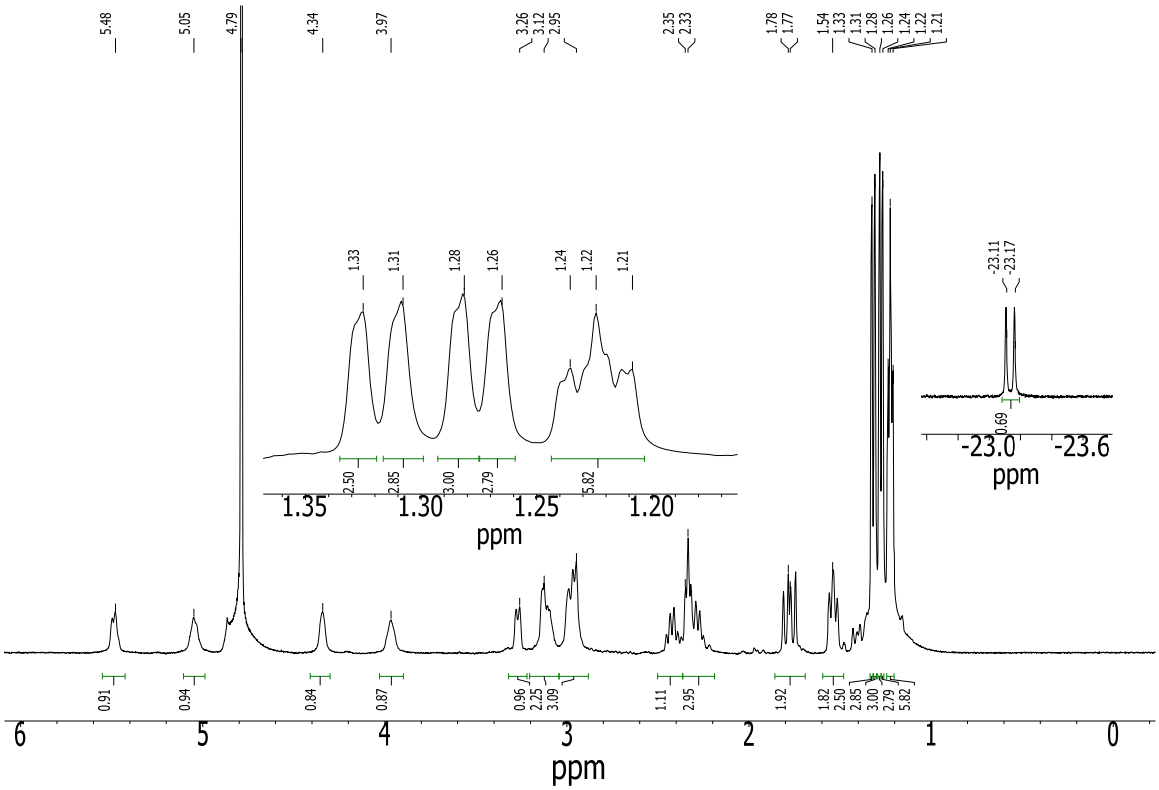

Figure S7. ^{1}H NMR of $L^{2}(H_2O)RhH^{2+}$, 600 MHz, D_2O. Left inset: ligand-CH_3 groups. Right inset: Rh-H signal. Signals at 5.05 ppm and 5.48 ppm are for exchangeable N-H protons.

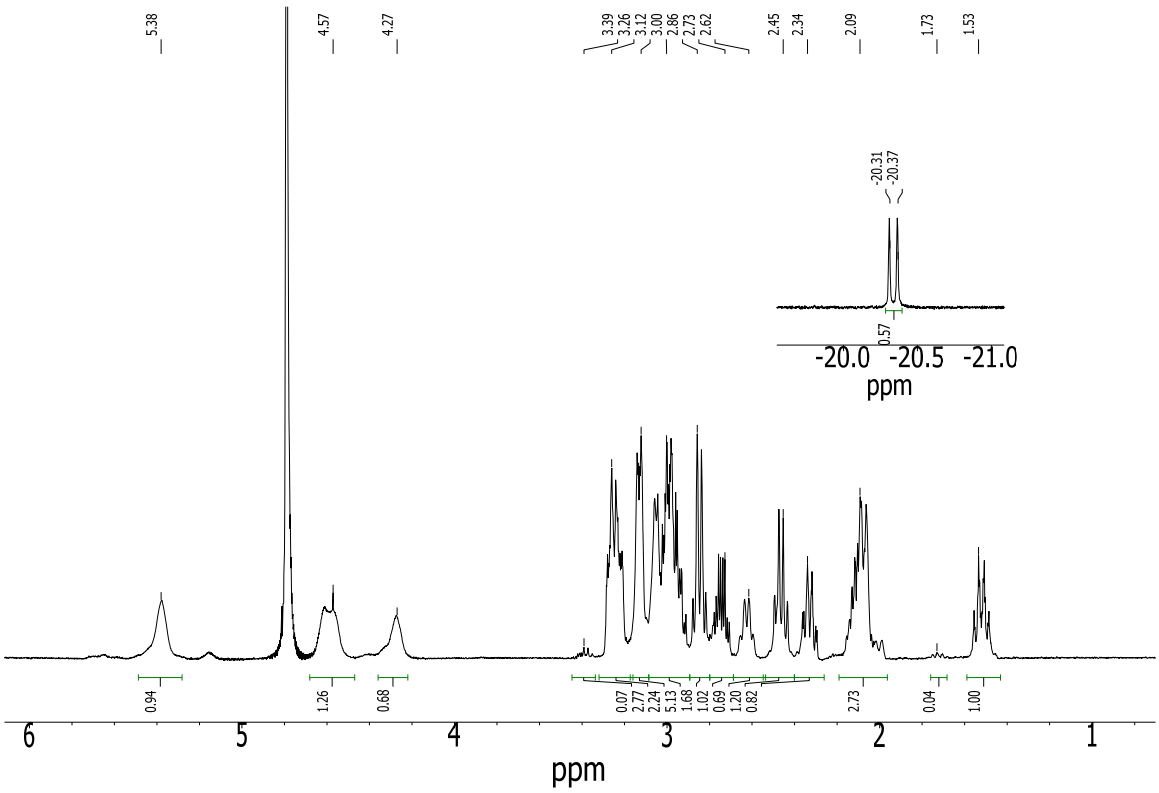

Figure S8. ^{1}H NMR of $L^{1}RhH^{2+}$, 600 MHz, D_2O.